Al-TiO_2 Composite-Modified Single-Layer Graphene as an Efficient Transparent Cathode for Organic Solar Cells

Di Zhang, Fengxian Xie, Peng Lin, and Wallace C. H. Choy*

Department of Electrical and Electronic Engineering, The University of Hong Kong, Pokfulam Road, Hong Kong

ABSTRACT

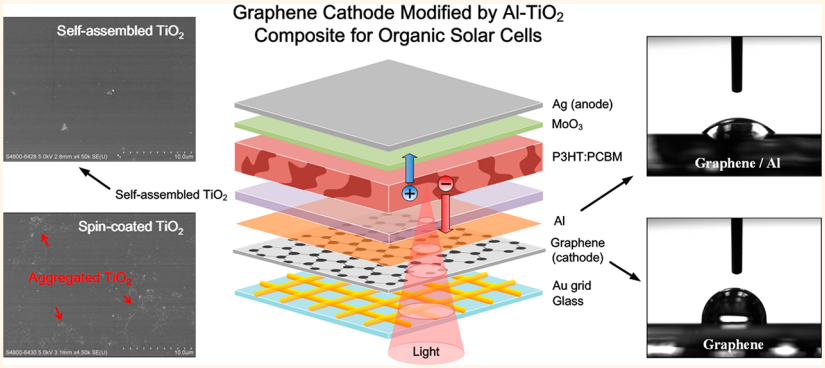

While there are challenges in tuning the properties of graphene (surface wettability, work function alignment, and carrier transport) for realizing an efficient graphene cathode in organic solar cells (OSCs), we propose and demonstrate using an Al-TiO_2 composite to modify single-layer graphene as an efficient cathode for OSCs. To unveil the contributions of the composite in addressing the aforementioned challenges, the evaporated aluminum nanoclusters in the composite benefit the graphene cathode by simultaneously achieving two roles of improving its surface wettability for subsequent TiO_2 deposition and reducing its work function to offer better energy alignment. To address challenges related to charge transport, solution-processed TiO_2 with excellent electron transport can offer charge extraction enhancement to the graphene cathode, which is essential to efficient devices. However, it is a well-known issue for methods such as spin-coating to produce uniform films on the initially hydrophobic graphene, even with improved wettability. The undesirable morphology of TiO_2 by such methods considerably inhibits its effectiveness in enhancing charge extraction. We propose a self-assembly method to deposit the solution-processed TiO_2 on the Al-covered graphene for forming the Al-TiO_2 composite. Compared with spin-coating, the self-assembly method is found to achieve more uniform coating on the graphene surface, with highly controllable thickness. Consequently, the graphene cathode modified with the Al-TiO_2 composite in inverted OSCs gives rise to enhanced power conversion efficiency of 2.58%, which is 2-fold of the previously best reported efficiency (1.27%) for graphene cathode OSCs, reaching ~75% performance of control devices using indium tin oxide.

KEYWORDS: organic solar cells · efficient graphene cathode · aluminum nanoclusters · titanium oxide · self-assembly film formation

Graphene, which is a single sheet composed of hexagonally arranged carbon atoms, has attracted extensive research interests.[1] Of the wide range of applications deemed promising, a flexible graphene transparent electrode for organic solar cells (OSCs) is quite attractive due to its excellent optical, electronic, and mechanical properties. One of the commonly utilized transparent electrodes in organic optoelectronics is indium tin oxide (ITO), which is relatively expensive and chemically unstable.[2,3] Moreover, ITO is rather brittle,[4] which is not inherently compatible with the flexibility nature of organic materials. Being only one atom thick, graphene has uniform white light transmittance of over 97%, with a negligible reflectance of <0.1%.[5] It has recently been reported that chemically doped large-area graphene can be readily

* Address correspondence to chchoy@eee.hku.hk.

Received for review December 18, 2012 and accepted January 17, 2013.

Published online
10.1021/nn3058399

© XXXX American Chemical Society

fabricated by a roll-to-roll method, with low sheet resistance (30 Ω sq^{-1}) comparable to that of ITO.[6] With the advances in solution-processed fabrication of chemically reduced graphene,[7,8] it is promising that large-area, high-quality graphene with low synthesis costs will soon be available. Furthermore, it has been demonstrated that the graphene electrode is more mechanically robust and flexible than ITO, showing superior performance under bending for flexible organic optoelectronic devices such as organic light-emitting diodes[9] and organic solar cells (OSCs).[10,11]

One of the key challenges is the interfacial modifications for graphene electrodes. In addition to being electrically conductive and optically transparent, the work function (WF) of the electrodes should be tuned by interfacial modifications in accordance with the molecular orbital of the donor or the acceptor, in order to minimize energy barriers at the anode or cathode, respectively. For graphene anodes, graphene oxide,[12] poly(3,4-ethylenedioxythiophene):poly(styrenesulfonate) (PEDOT:PSS),[11,13,14] and PEDOT/MoO_3 double layers[2] have been shown as effective hole transport layers (HTLs), with efficient power conversion efficiency (PCE) of 2.5−2.7% recorded. Previously, we have also reported PEDOT-free gold nanoclusters as an effective HTL for a multilayer graphene anode.[15] Nevertheless, there is yet to be efficient OSCs using graphene cathodes. Jo *et al.* reported an inverted OSC using a graphene cathode modified by a polyfluorene interfacial dipole layer, which yielded a PCE of 1.23%.[16] Doped with alkali carbonate salt, a graphene/carbon nanotube cathode for inverted OSCs was reported by Huang *et al.*, with 1.27% PCE.[17] At present, the highest reported PCE for graphene cathode OSCs is still below 1.3%.[16−18] The realization of an efficient graphene cathode is crucial to the versatility and design flexibility of graphene transparent electrodes.

Meanwhile, inorganic transition metal oxides (p-type and n-type) have newly emerged as promising candidates for fulfilling the role of efficient interface layers.[19] Oxides such as MoO_3, V_2O_5, and WO_3 are good hole transport materials,[20−23] whereas ones such as TiO_2 and ZnO are good electron transport materials.[24,25] Recently, efficient interface layers using solution-processed metal oxides have been reported.[23,25−27] However, for solution processes, graphene electrodes need to overcome its hydrophobic surface, which is initially not compatible with deposition methods such as spin-coating.[28] Therefore, it is highly desirable to develop effective interfacial modifications for a graphene cathode which can address its surface wettability issue while enabling efficient OSC devices.

In this work, we propose to introduce the composite interface layer of aluminum (Al) nanoclusters and titanium oxide (TiO_2) to modify single-layer graphene (SLG) as a transparent cathode for inverted OSCs. Previously, WF lowering was observed on multilayer graphene samples by using a subnanometer AlO_x layer.[29] Differently, the Al-TiO_2 composite in this work simultaneously provides a series of interfacial modifications on the graphene cathode, which enable efficient device operation of graphene cathode OSCs. As characterized by contact angle measurement and ultraviolet photoelectron spectroscopy (UPS), the thin Al nanoclusters in the Al-TiO_2 composite significantly improve the surface wettability of SLG, while reducing its WF for better energy alignment and electron extraction. Furthermore, solution-processed TiO_2 as an efficient electron transport material in the Al-TiO_2 composite is essential to provide further charge extraction enhancement on the Al-covered SLG. Its effectiveness for enhancing electron transport, however, may be limited by the poor uniformity of films deposited on the hydrophobic graphene. To address this well-known issue related to the graphene surface, we propose a self-assembly method which can readily deposit the subsequent TiO_2 solution on the Al-covered SLG. Compared to spin-coating, our self-assembly method can achieve more uniform and controllable coating of TiO_2 films on the initially hydrophobic SLG surface. As a result, the SLG cathode modified with the Al-TiO_2 composite layer yields an efficient PCE of 2.58% in inverted OSCs, which is higher than the previously reported efficiencies.

RESULTS AND DISCUSSION

Al Nanoclusters on Graphene: Wettability Enhancement and Work Function Tuning. SLG films were transferred to a glass substrate assisted by poly(methyl methacrylate) (PMMA).[30] Figure 1a is the scanning electron microscope (SEM) image of transferred SLG on the glass substrate. The SLG samples were characterized optically and electrically, with optical transmittance (Figure 1b, black line) of 96.0% at 500 nm and sheet resistance (SR) of ∼1.2 kΩ sq^{-1}. The high and uniform transmittance confirms the graphene samples to be single layer.

Nevertheless, conformal coating of various solution-processed interface layers on graphene remains a challenging issue due to its intrinsically hydrophobic surface. For solution-processed electron transport layers (ETLs) such as TiO_2, we find that the solutions cannot be directly spin-coated on the SLG surface, which results in poor device performance similar to that of device directly made without ETL spin-coating (both cases PCE ∼ 0).

Here, we choose to improve the wettability of the SLG surface by thermally evaporating very thin Al nanoclusters as the first step of interfacial modifications for the graphene cathode by the Al-TiO_2 composite. For pristine SLG, the average contact angle is large (95.7°, summarized in Table 1), suggesting a very hydrophobic surface. Interestingly, when thin Al nanoclusters (∼0.5 nm) are evaporated onto SLG samples, the surface contact angle considerably reduces to 48.0° (Table 1), indicating largely improved surface wettability. Figure 2a,b illustrates the improvement

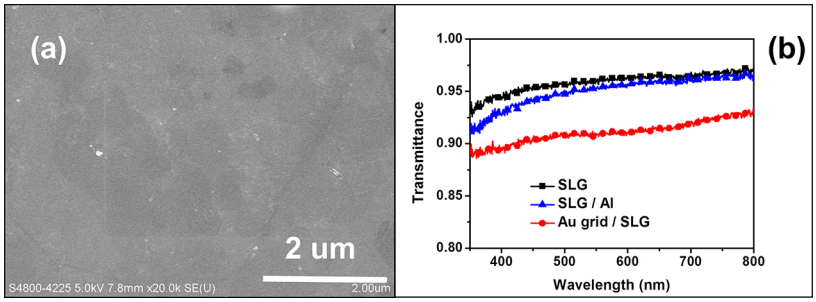

Figure 1. (a) SEM image of SLG film on the glass substrate and (b) optical transmittance of SLG, SLG/Al (0.5 nm), and Au grid/SLG samples.

TABLE 1. Surface Contact Angles of SLG Samples Applied with Different Treatments (with and without Al Evaporation (0.5 nm), and/or UVO Treatment)[a]

samples	contact angle (deg)
SLG	95.7 ± 5.2
SLG/Al	48.0 ± 5.6
SLG + UVO (1 min)	89.0 ± 8.8
SLG + UVO (10 min)	51.2 ± 3.7
SLG/Al + UVO (1 min)	44.6 ± 3.7

[a] Each sample is measured in three locations across the sample surface.

accordingly. It should also be noted that the Al evaporation on SLG only introduces a slight decrease in optical transparency, to 94.8% transmittance at 500 nm, as shown in Figure 1b (blue line).

It has been shown that the uniformity of aqueous PEDOT:PSS on graphene can be improved by applying ultraviolet-ozone (UVO) or O_2 plasma treatment in advance, *via* introducing hydroxyl (OH) and carbonyl (C=O) groups.[28,31] Sufficient length of duration is usually required for direct UVO treatment to fully convert the surface, as it is common to apply UVO of 10−15 min on ITO while multilayer graphene (MLG) treated with UVO of 6−10 min has been reported.[15,28] For reference, the contact angles of SLG samples applied with different durations of UVO were measured (Table 1). We find that UVO of short duration (∼1 min) can only moderately improve the overall wettability of SLG samples (contact angle reduced from 95.7 to 89.0°). While long duration (10 min) of UVO can reduce the contact angle to 51.2°, the wettability enhancement is less optimal than the case of simply depositing 0.5 nm Al (with contact angle of only 48.0°). The wettability of SLG/Al samples can be further improved by a short (1 min) UVO exposure for a smaller contact angle of 44.6°. Importantly, oxygen groups introduced by extended UVO or O_2 plasma treatment tend to disrupt the aromatic structures of graphene, resulting in structure damage and rapid decrease in conductivity.[28,32] The detrimental effect is even more prominent for SLG than MLG, as the thinner graphene with a single layer is more prone to be compromised by the strong oxidation. Indeed, we observe considerable increase in the SR of SLG treated with 10 min of UVO, from ∼1.2 to >10 kΩ sq^{-1}. The rapid decrease in conductivity by extended UVO treatment is detrimental to the OSC device, as will be discussed later. Meanwhile, the spontaneous wettability improvement of the SLG/Al surface without UVO treatment may be attributed to the absorbed oxygen and formation of AlO_x at the graphene/Al interface.[29] Consequently, compared to the direct oxidation of SLG by UVO, the ambient oxidation with thin Al nanoclusters on SLG provides significantly better wettability enhancement, without compromising the conductivity of SLG for OSC performance.

Importantly, besides improving the surface wettability, the thin Al nanoclusters on SLG contribute to a more energetically favorable cathode interface by lowering the WF of graphene for better energy alignment with the organic acceptor. Figure 3 shows the UPS spectra of SLG samples with different Al thickness. For pristine SLG, the measured WF is 4.56 eV, which is largely mismatched with the lowest unoccupied molecular orbital (LUMO) of acceptor $PC_{61}BM$ ([6,6]-phenyl-C61-butyric acid methyl ester, 4.2 eV[27]) in OSCs for efficient electron transport. The secondary electron cutoff for the SLG shifts toward a high binding energy with only 0.1 nm Al deposited and shifts further when Al nanoclusters of 0.5 nm are evaporated. The resulting WFs are considerably reduced to 4.36 and 4.14 eV. As a result, energy alignment between SLG and the PCBM acceptor is considerably improved at the cathode interface by Al nanoclusters for facilitating electron extraction in OSCs, as schematically shown in Figure 4a.

Charge Extraction Enhancement by Self-Assembled TiO_2: Uniform Morphology and Controllable Coating. Even with the Al nanoclusters modifying the surface and energetic properties, the graphene cathode cannot effectively transport and extract electrons for OSC devices. Therefore, a two-step composite interface layer is required, in which an electron transport layer is further deposited on the Al-covered SLG to enhance electron extraction. Solution-processed TiO_2 nanocrystals are chosen in this work due to the excellent electron transport demonstrated in ITO devices while being capable of large-area, low-cost applications.[33] Nevertheless,

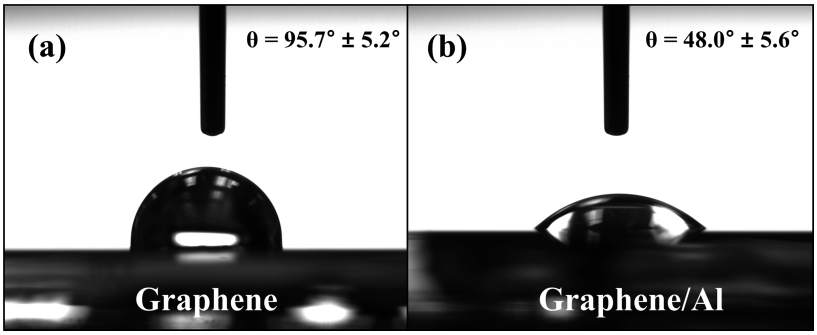

Figure 2. Surface contact angles of (a) SLG and (b) SLG/Al (~0.5 nm) samples.

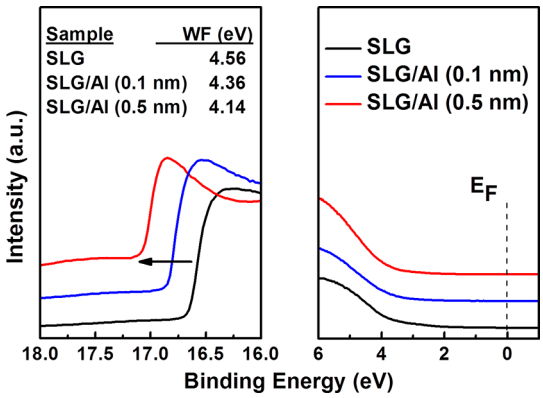

Figure 3. UPS spectra and calculated WFs of SLG and SLG/Al (0.1 and 0.5 nm) samples.

depositing conformal and uniform films from solutions on the initially hydrophobic graphene surface is a well-known challenging issue, which may severely affect device performances. Indeed, we find that, using conventional spin-coating, TiO_2 films deposited on Al-covered SLG exhibit defective surface morphology, which results in rather poor performances for OSC devices, as will be discussed later.

Here, we introduce a self-assembly method to further deposit solution-processed TiO_2 on the Al-covered SLG, in order to achieve uniform coating and enable efficient device performance. The TiO_2 nanocrystals are strategically dispersed in ethanol solution due to its relatively low surface tension and viscosity, indicating that the solution can form good contact with the electrode and spread uniformly. The weak intermolecular interactions—hydrogen bond in ethanol—are responsible for nanoparticles aligning and arranging orderly.

In order to facilitate TiO_2 nanocrystal alignment, we quickly cover the SLG/Al substrate by a small Petri dish after casting the TiO_2 solution onto the substrate. The ethanol solution then gradually spreads to cover the SLG surface. The evaporation rate of the solvent is controlled within the containment, while the whole process takes about 30 min. It is worth noting that the evaporated Al is an important prerequisite for the self-assembly process, as we find that the TiO_2 solution cannot spread on the SLG surface with otherwise poor wettability as discussed in the previous section.

As a result, using the self-assembly method, TiO_2 films with good uniformity and highly controllable thickness can be readily deposited on the SLG/Al surface, which is essential for effective charge extraction enhancement and efficient device performance. Examined by SEM, we compare the surface morphology of TiO_2 films coated on the SLG/Al surface by spin-coating and self-assembly methods using identical TiO_2 solutions, as shown in Figure 5. We find that defect sites such as TiO_2 aggregations are typical of spin-coated films on SLG/Al, which are likely associated with the rapid solvent evaporation process not allowing gradual nanocrystal alignment (Figure 5a). Such undesired aggregations are much fewer on TiO_2 films deposited by the self-assembly method, which yields more uniform coating of the films (Figure 5b). Furthermore, TiO_2 films coated by the self-assembly process are also highly controllable, with thickness ranging from ~10 to over 100 nm, readily obtained by varying TiO_2 concentration and solution casting volume. In comparison, controllable thickness of TiO_2 film on SLG/Al is difficult for the conventional method of spin-coating. Our results show that spin-coated TiO_2 film on SLG is rather thin with limited thickness (usually <20 nm regardless of spin-coating settings), even with the improved wettability by Al nanoclusters. Figure 6 shows a thickness comparison measured by cross-section SEM between spin-coated and self-assembled TiO_2 films on SLG/Al made from TiO_2 solution of the same concentration. While self-assembled TiO_2 film coated on SLG/Al is quite thick (~67.5 nm, 20 μL solution-casted), spin-coated TiO_2 film on the same substrate using identical solution is still very thin (~19.0 nm, 80 μL solution-casted), even for a rather slow spin speed (1000 rpm). While multiple spin-coating processes may increase the coating thickness, the procedure is not easily controlled and the thickness only moderately increases (see Figure S1 in Supporting Information), not to mention the surface morphology of the film which may be compromised by the repeated process.

Device Performance of OSCs Using the Graphene Cathode. To better show the contributions of the composite-modified cathode to the OSC device performances, the SLG cathode modified with the Al-TiO_2 composite interface layer was incorporated into poly(3-hexylthiophene)

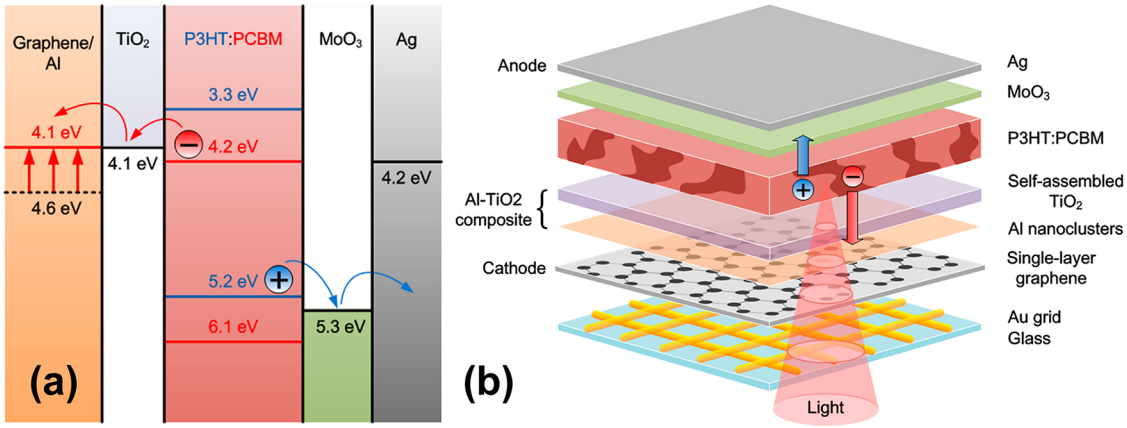

Figure 4. (a) Flat-band energy diagram of organic solar cells using the graphene cathode modified by the Al-TiO_2 composite. The work function decrease from pristine graphene (denoted by black dashed line, 4.6 eV) to graphene/Al (denoted by red solid line, 4.1 eV) is indicated by upward red arrows. (b) Device structure of inverted organic solar cells using the graphene cathode shown in (a).

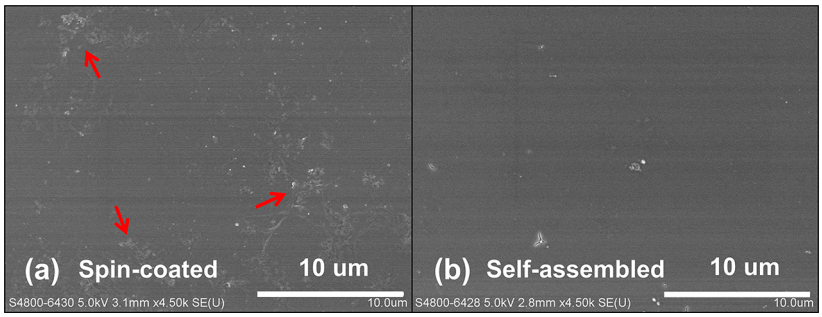

Figure 5. Surface SEM images of TiO_2 films coated on the SLG/Al surface by (a) spin-coating and (b) self-assembly method, using identical TiO_2 solutions. The visible TiO_2 aggregations on spin-coated film are marked by arrows.

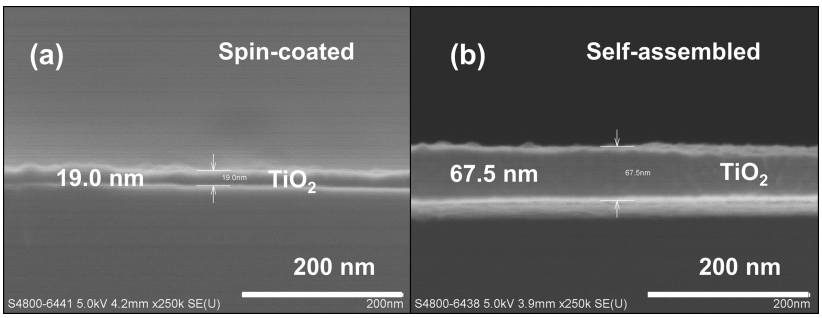

Figure 6. Cross-section SEM images of TiO_2 films coated on the SLG/Al surface by (a) spin-coating and (b) self-assembly method, using identical TiO_2 solutions.

(P3HT):$PC_{61}BM$ inverted OSCs (device structure schematically shown in Figure 4b). The device performances of a representative set of inverted OSCs with the device structure of glass/cathode/P3HT:$PC_{61}BM$ (220 nm)/MoO_3 (14 nm)/Ag (100 nm) are shown in Figure 7 and summarized in Table 2. While the surface wettability of SLG can be moderately improved by extended UVO for subsequent self-assembled TiO_2 deposition, the conductivity of graphene compromised in the process results in poor device performances (PCE ~ 0 for 10 min UVO). Using evaporated Al nanoclusters and self-assembled TiO_2 as the Al-TiO_2 composite ETL for the SLG cathode, the optimized inverted SLG/Al-TiO_2 OSCs reach an average PCE of 1.59%. The Al-TiO_2 composite demonstrates its effectiveness as an ETL for the graphene cathode by exhibiting good open-circuit voltage (V_{OC}) of 0.58 V and short-circuit current density (J_{SC}) of 7.85 mA/cm^2. As previously stated, the evaporated Al nanoclusters considerably improve the surface wettability and reduce the WF of SLG cathode, which benefit subsequent film deposition and energy alignment at the cathode interface, respectively. The thickness of Al nanoclusters is found to be critical to device performances (shown in Table S1 in Supporting Information), as thicker Al evaporation may introduce excessive insulating AlO_x

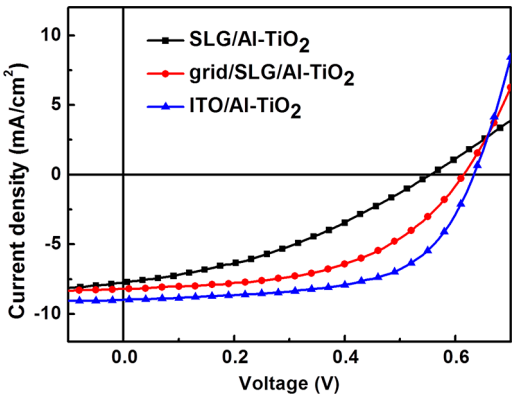

Figure 7. $J-V$ characteristics of a representative set of inverted PSCs with the device structure of cathode/P3HT:$PC_{61}BM$ (220 nm)/MoO_3 (14 nm)/Ag (100 nm).

TABLE 2. Device Performance of a Representative Set of Inverted PSCs with the Device Structure of Cathode/P3HT:$PC_{61}BM$ (220 nm)/MoO_3 (14 nm)/Ag (100 nm)

cathode structure	J_{SC} (mA/cm^2)	V_{OC} (V)	FF (%)	PCE (%)
SLG/Al-TiO_2	7.85 ± 0.24	0.58 ± 0.02	35.0 ± 3.2	1.59 ± 0.08
grid/SLG/Al-TiO_2	8.55 ± 0.62	0.60 ± 0.01	50.1 ± 2.5	2.58 ± 0.09
ITO/Al-TiO_2	9.11 ± 0.25	0.63 ± 0.00	60.1 ± 0.3	3.45 ± 0.09
SLG/Al/spin-coated TiO_2	1.80 ± 0.65	0.30 ± 0.04	25.2 ± 0.5	0.14 ± 0.07
grid only/Al-TiO_2	1.31 ± 0.56	0.61 ± 0.01	33.2 ± 0.5	0.27 ± 0.11
SLG/TiO_2 + UVO (10 min)				0

at the cathode interface. The Al nanocluster evaporation is followed by TiO_2 deposition by the self-assembly method, which can achieve uniform and controllable coating for effective electron extraction enhancement. In comparison, OSCs made from spin-coated TiO_2 on the SLG/Al cathode generally showed poor V_{OC} (0.30 V), due to the defective surface morphology of TiO_2 films coated on SLG, as observed by SEM (Figure 5a).

Because of the high SR of intrinsic SLG itself (1.2 kΩ sq^{-1}), the OSC devices suffer from additional series resistance from the graphene cathode, which significantly limits the fill factor (FF) of the device (35.0%). Several methods have been reported to decrease the SR of pristine graphene films, such as doping chemically by acids, by gold particles, or by metal nanowires.[2,6,11,31,34,35] For further device optimization, we deposit metallic (Au) grids onto the glass substrates prior to SLG transfer, which act as the electrical backbone for the SLG electrode.[36] The Au grids are beneath SLG films and are not in direct contact with the cathode interface. The deposition of the Au grids is detailed in the Experimental Section. The grid/SLG electrode shows largely enhanced conductivity (SR = 20−30 Ω sq^{-1}) comparable to ITO (SR = 20 Ω sq^{-1}), while remaining optically transparent (90.7% transmittance at 500 nm, Figure 1b, red line). By using Au grids to substantially increase the conductivity of SLG cathodes, we observe a remarkable increase in FF (from 35.0 to 50.1%) and J_{SC} (from 7.85 to 8.55 mA/cm^2). As a result, the average PCE for inverted OSCs using the SLG/Al-TiO_2 cathode is improved significantly to an efficient 2.58%, with desirable FF and V_{OC} (0.60 V). Interestingly, the average PCE of the optimized SLG cathode OSCs reaches ∼75% of control devices using the ITO cathode and identical Al-TiO_2 composite interface layer (average PCE = 3.45%).

It should be noted that, with the addition of Au grids underneath graphene, the thickness of the Au grids (50 nm) may introduce uneven morphology for thin TiO_2 coating, which was optimized from graphene OSCs without the grids. Therefore, a thicker TiO_2 layer, which can offset the height difference between the grid-covered and noncovered surface, is utilized to improve morphology and optimize the performance. By increasing TiO_2 thickness, we observed considerably improved performance in OSCs using Au grids (as shown in Table S2 in Supporting Information). In order to confirm that Au grids merely function as conductivity enhancement for the SLG cathode, grid-only OSCs were constructed using Au grids as the intended cathode modified with an Al-TiO_2 layer, without the SLG between. The grid-only OSCs exhibited very small J_{SC} (1.31 mA/cm^2) due to the large grid spacing and poor FF (33.2%), possibly due to the mismatched WF of Au (∼5.2 eV). The resulting PCE of 0.27% confirms the significance of the SLG cathode in the OSC devices.

CONCLUSIONS

In conclusion, we have proposed and demonstrated the interface engineering of graphene as a transparent cathode for inverted OSCs by an Al-TiO_2 composite interface layer. The thin Al nanoclusters in the Al-TiO_2 composite simultaneously improve the surface wettability of SLG for subsequent TiO_2 deposition and reduce its WF for better energy alignment. We introduce a self-assembly approach for TiO_2 deposition and careful selection of ethanol solvent to form TiO_2 films on SLG with uniform surface morphology and highly controllable thickness. The two-step modifications form an optimized Al-TiO_2 composite interface layer for SLG to function as an effective cathode for OSC devices. As a result, the transparent SLG cathode modified with the Al-TiO_2 composite layer yields an optimized PCE of 2.58% in inverted OSCs, demonstrating more efficient performances than those of previously reported.

EXPERIMENTAL SECTION

Materials. SLG films synthesized by a chemical vapor deposition (CVD) process[37] on copper foils were purchased from Graphene Supermarket. Copper foils were etched away by iron(III) chloride solution (20 mg/mL), while SLG films were supported and transferred to glass substrates by PMMA.[30]

The ligand-free anatase TiO_2 nanocrystals were synthesized by a non-aqueous method,[38] with the TiO_2 nanoparticles being ~4 nm in size and dispersed in ethanol.

Device Fabrication. Gold grids were thermally evaporated onto the glass substrates prior to SLG transfer to enhance the conductivity of the SLG cathode, which are beneath SLG films and are not in direct contact with the cathode interface. The Au grids are 50 nm thick, with line width of 10 μm and grid spacing of 200 μm. Aluminum nanoclusters were thermally evaporated onto SLG samples under 6×10^{-4} Pa, with thickness monitored by a quartz sensor. After Al evaporation, the SLG/Al samples were treated with short UVO (1 min). The Al-TiO_2 composite layer on SLG was finished by depositing solution-processed TiO_2 nanocrystals using a self-assembly method.[33] After the self-assembly/spin-coating process, all TiO_2 films (30−40 nm) were annealed at 150 °C for 10 min on a hot plate in ambient conditions. The prepared SLG samples were then transferred into a nitrogen-filled glovebox for spin-coating the blend of poly(3-hexylthiophene) (P3HT) and [6,6]-phenyl-C61-butyric acid methyl ester ($PC_{61}BM$) with 1:1 weight ratio (20 mg/mL each dissolved in 1,2-dichlorobenzene). Before annealing at 130 °C for 10 min on a hot plate, solvent annealing is utilized as described elsewhere.[39] MoO_3 (14 nm)/Ag (100 nm) was thermally evaporated as the top anode, which defines the device area as 0.04−0.06 cm^2. The final device structure was SLG/Al-TiO_2/P3HT:$PC_{61}BM$ (220 nm)/MoO_3 (14 nm)/Ag (100 nm). For reference, the ITO cathode using an identical Al-TiO_2 composite ETL was incorporated in the OSC device with the structure of ITO/Al-TiO_2/P3HT:$PC_{61}BM$/MoO_3/Ag.

Characterizations. Current density−voltage ($J-V$) characteristics were measured by using a Keithley 2635 sourcemeter and ABET AM1.5G solar simulator. UPS measurement was carried out by using a He discharged lamp (He I 21.22 eV, Kratos Analytical). SEM images were obtained using a Hitachi S-4800 FEG scanning electron microscope.

Conflict of Interest: The authors declare no competing financial interest.

Acknowledgment. This work is supported by University Grant Council of the University of Hong Kong (Grant Nos. 10401466 and 201111159062), and the General Research Fund (Grants Nos. HKU712010E and HKU711612E), and the RGC-NSFC grant (N_HKU709/12) from the Research Grants Council of Hong Kong Special Administrative Region, China. D.Z. would like to acknowledge Hong Kong Ph.D. Fellowship from the Research Grants Council of Hong Kong. We acknowledge the help of Erica Chang and Tony Feng for measuring contact angle of our samples, and Xuanhua Li for conducting SEM measurement.

Supporting Information Available: Thickness increment of TiO_2 layer spin-coated multiple times (Figure S1) and device performance of inverted PSCs using SLG/Al-TiO_2 cathode with different Al thickness (Table S1) and different TiO_2 thickness (Table S2). This material is available free of charge *via* the Internet at http://pubs.acs.org.

REFERENCES AND NOTES

1. Novoselov, K.; Geim, A.; Morozov, S.; Jiang, D.; Zhang, Y.; Dubonos, S.; Grigorieva, I.; Firsov, A. Electric Field Effect in Atomically Thin Carbon Films. *Science* **2004**, *306*, 666–669.
2. Wang, Y.; Tong, S. W.; Xu, X. F.; Özyilmaz, B.; Loh, K. P. Interface Engineering of Layer-by-Layer Stacked Graphene Anodes for High-Performance Organic Solar Cells. *Adv. Mater.* **2011**, *23*, 1514–1518.
3. Schlatmann, A. Indium Contamination from the Indium-Tin-Oxide Electrode in Polymer Light-Emitting Diodes. *Appl. Phys. Lett.* **1996**, *69*, 1764.
4. Chen, Z.; Cotterell, B.; Wang, W.; Guenther, E.; Chua, S.-J. A Mechanical Assessment of Flexible Optoelectronic Devices. *Thin Solid Films* **2001**, *394*, 201–205.
5. Nair, R.; Blake, P.; Grigorenko, A.; Novoselov, K.; Booth, T.; Stauber, T.; Peres, N.; Geim, A. Fine Structure Constant Defines Visual Transparency of Graphene. *Science* **2008**, *320*, 1308.
6. Bae, S.; Kim, H.; Lee, Y.; Xu, X.; Park, J.-S.; Zheng, Y.; Balakrishnan, J.; Lei, T.; Ri Kim, H.; Song, Y. I.; *et al.* Roll-to-Roll Production of 30-Inch Graphene Films for Transparent Electrodes. *Nat. Nanotechnol.* **2010**, *5*, 574–578.
7. Sire, C.; Ardiaca, F.; Lepilliet, S.; Seo, J.-W. T.; Hersam, M. C.; Dambrine, G.; Happy, H.; Derycke, V. Flexible Gigahertz Transistors Derived from Solution-Based Single-Layer Graphene. *Nano Lett.* **2012**, *12*, 1184–1188.
8. Wöbkenberg, P. H.; Eda, G.; Leem, D. S.; de Mello, J. C.; Bradley, D. D. C.; Chhowalla, M.; Anthopoulos, T. D. Reduced Graphene Oxide Electrodes for Large Area Organic Electronics. *Adv. Mater.* **2011**, *23*, 1558–1562.
9. Han, T. H.; Lee, Y.; Choi, M. R.; Woo, S. H.; Bae, S. H.; Hong, B. H.; Ahn, J. H.; Lee, T. W. Extremely Efficient Flexible Organic Light-Emitting Diodes with Modified Graphene Anode. *Nat. Photonics* **2012**, *6*, 105–110.
10. Gomez De Arco, L.; Zhang, Y.; Schlenker, C. W.; Ryu, K.; Thompson, M. E.; Zhou, C. Continuous, Highly Flexible, and Transparent Graphene Films by Chemical Vapor Deposition for Organic Photovoltaics. *ACS Nano* **2010**, *4*, 2865–2873.
11. Lee, S.; Yeo, J. S.; Ji, Y.; Cho, C.; Kim, D. Y.; Na, S. I.; Lee, B. H.; Lee, T. Flexible Organic Solar Cells Composed of P3HT: PCBM Using Chemically Doped Graphene Electrodes. *Nanotechnology* **2012**, *23*, 344013.
12. Lee, Y.-Y.; Tu, K.-H.; Yu, C.-C.; Li, S.-S.; Hwang, J.-Y.; Lin, C.-C.; Chen, K.-H.; Chen, L.-C.; Chen, H.-L.; Chen, C.-W. Top Laminated Graphene Electrode in a Semitransparent Polymer Solar Cell by Simultaneous Thermal Annealing/Releasing Method. *ACS Nano* **2011**, *5*, 6564–6570.
13. Hsu, C. L.; Lin, C. T.; Huang, J. H.; Chu, C. W.; Wei, K. H.; Li, L. J. Layer-by-Layer Graphene/TCNQ Stacked Films as Conducting Anodes for Organic Solar Cells. *ACS Nano* **2012**, *6*, 5031–5039.
14. Liu, Z.; Li, J.; Sun, Z.-H.; Tai, G.; Lau, S.-P.; Yan, F. The Application of Highly Doped Single-Layer Graphene as the Top Electrodes of Semitransparent Organic Solar Cells. *ACS Nano* **2011**, *6*, 810–818.
15. Zhang, D.; Choy, W. C. H.; Wang, C. C. D.; Li, X.; Fan, L.; Wang, K.; Zhu, H. Polymer Solar Cells with Gold Nanoclusters Decorated Multi-Layer Graphene as Transparent Electrode. *Appl. Phys. Lett.* **2011**, *99*, 223302.
16. Jo, G.; Na, S.-I.; Oh, S.-H.; Lee, S.; Kim, T.-S.; Wang, G.; Choe, M.; Park, W.; Yoon, J.; Kim, D.-Y.; *et al.* Tuning of a Graphene-Electrode Work Function To Enhance the Efficiency of Organic Bulk Heterojunction Photovoltaic Cells with an Inverted Structure. *Appl. Phys. Lett.* **2010**, *97*, 213301.
17. Huang, J. H.; Fang, J. H.; Liu, C. C.; Chu, C. W. Effective Work Function Modulation of Graphene/Carbon Nanotube Composite Films as Transparent Cathodes for Organic Optoelectronics. *ACS Nano* **2011**, *5*, 6262–6271.
18. Cox, M.; Gorodetsky, A.; Kim, B.; Kim, K. S.; Jia, Z.; Kim, P.; Nuckolls, C.; Kymissis, I. Single-Layer Graphene Cathodes for Organic Photovoltaics. *Appl. Phys. Lett.* **2011**, *98*, 123303.
19. Greiner, M. T.; Helander, M. G.; Tang, W.-M.; Wang, Z.-B.; Qiu, J.; Lu, Z.-H. Universal Energy-Level Alignment of Molecules on Metal Oxides. *Nat. Mater.* **2012**, *11*, 76–81.
20. Tao, C.; Ruan, S.; Zhang, X.; Xie, G.; Shen, L.; Kong, X.; Dong, W.; Liu, C.; Chen, W. Performance Improvement of Inverted Polymer Solar Cells with Different Top Electrodes by Introducing a MoO_3 Buffer Layer. *Appl. Phys. Lett.* **2008**, *93*, 193307.
21. Tao, C.; Ruan, S.; Xie, G.; Kong, X.; Shen, L.; Meng, F.; Liu, C.; Zhang, X.; Dong, W.; Chen, W. Role of Tungsten Oxide in Inverted Polymer Solar Cells. *Appl. Phys. Lett.* **2009**, *94*, 043311.
22. Huang, J.-S.; Chou, C.-Y.; Liu, M.-Y.; Tsai, K.-H.; Lin, W.-H.; Lin, C.-F. Solution-Processed Vanadium Oxide as an Anode Interlayer for Inverted Polymer Solar Cells Hybridized with ZnO Nanorods. *Org. Electron.* **2009**, *10*, 1060–1065.
23. Meyer, J.; Khalandovsky, R.; Görrn, P.; Kahn, A. MoO_3 Films Spin-Coated from a Nanoparticle Suspension for Efficient Hole-Injection in Organic Electronics. *Adv. Mater.* **2011**, *23*, 70–73.
24. Park, M.-H.; Li, J.-H.; Kumar, A.; Li, G.; Yang, Y. Doping of the Metal Oxide Nanostructure and Its Influence in Organic Electronics. *Adv. Funct. Mater.* **2009**, *19*, 1241–1246.

25. Hau, S. K.; Yip, H.-L.; Baek, N. S.; Zou, J.; O'Malley, K.; Jen, A. K. Y. Air-Stable Inverted Flexible Polymer Solar Cells Using Zinc Oxide Nanoparticles as an Electron Selective Layer. *Appl. Phys. Lett.* **2008**, *92*, 253301.
26. Lee, Y.-J.; Yi, J.; Gao, G. F.; Koerner, H.; Park, K.; Wang, J.; Luo, K.; Vaia, R. A.; Hsu, J. W. P. Low-Temperature Solution-Processed Molybdenum Oxide Nanoparticle Hole Transport Layers for Organic Photovoltaic Devices. *Adv. Energy Mater.* **2012**, *2*, 1193–1197.
27. You, J.; Chen, C.-C.; Dou, L.; Murase, S.; Duan, H.-S.; Hawks, S. A.; Xu, T.; Son, H. J.; Yu, L.; Li, G.; *et al.* Metal Oxide Nanoparticles as an Electron-Transport Layer in High-Performance and Stable Inverted Polymer Solar Cells. *Adv. Mater.* **2012**, *24*, 5267–5272.
28. Wang, Y.; Chen, X.; Zhong, Y.; Zhu, F.; Loh, K. P. Large Area, Continuous, Few-Layered Graphene as Anodes in Organic Photovoltaic Devices. *Appl. Phys. Lett.* **2009**, *95*, 063302.
29. Yi, Y.; Choi, W. M.; Kim, Y. H.; Won Kim, J.; Kang, S. J. Effective Work Function Lowering of Multilayer Graphene Films by Subnanometer Thick AlO_x Overlayers. *Appl. Phys. Lett.* **2011**, *98*, 013505.
30. Reina, A.; Son, H.; Jiao, L.; Fan, B.; Dresselhaus, M. S.; Liu, Z.; Kong, J. Transferring and Identification of Single- and Few-Layer Graphene on Arbitrary Substrates. *J. Phys. Chem. C* **2008**, *112*, 17741–17744.
31. Hyesung, P.; Rowehl, J. A.; Kim, K. K.; Bulovic, V.; Kong, J. Doped Graphene Electrodes for Organic Solar Cells. *Nanotechnology* **2010**, *21*, 505204.
32. Shin, Y. J.; Wang, Y.; Huang, H.; Kalon, G.; Wee, A. T. S.; Shen, Z.; Bhatia, C. S.; Yang, H. Surface-Energy Engineering of Graphene. *Langmuir* **2010**, *26*, 3798–3802.
33. Zhang, D.; Choy, W. C. H.; Xie, F.-x.; Li, X. Large-Area, High-Quality Self-Assembly Electron Transport Layer for Organic Optoelectronic Devices. *Org. Electron.* **2012**, *13*, 2042–2046.
34. Güneş, F.; Shin, H. J.; Biswas, C.; Han, G. H.; Kim, E. S.; Chae, S. J.; Choi, J. Y.; Lee, Y. H. Layer-by-Layer Doping of Few-Layer Graphene Film. *ACS Nano* **2010**, *4*, 4595.
35. Kholmanov, I. N.; Magnuson, C. W.; Aliev, A. E.; Li, H.; Zhang, B.; Suk, J. W.; Zhang, L. L.; Peng, E.; Mousavi, S. H.; Khanikaev, A. B.; *et al.* Improved Electrical Conductivity of Graphene Films Integrated with Metal Nanowires. *Nano Lett.* **2012**, *12*, 5679–5683.
36. Zhu, Y.; Sun, Z.; Yan, Z.; Jin, Z.; Tour, J. M. Rational Design of Hybrid Graphene Films for High-Performance Transparent Electrodes. *ACS Nano* **2011**, *5*, 6472–6479.
37. Li, X.; Cai, W.; An, J.; Kim, S.; Nah, J.; Yang, D.; Piner, R.; Velamakanni, A.; Jung, I.; Tutuc, E.; *et al.* Large-Area Synthesis of High-Quality and Uniform Graphene Films on Copper Foils. *Science* **2009**, *324*, 1312–1314.
38. Jensen, G. V.; Bremholm, M.; Lock, N.; Deen, G. R.; Jensen, T. R.; Iversen, B. B.; Niederberger, M.; Pedersen, J. S.; Birkedal, H. Anisotropic Crystal Growth Kinetics of Anatase TiO_2 Nanoparticles Synthesized in a Nonaqueous Medium. *Chem. Mater.* **2010**, *22*, 6044–6055.
39. Li, G.; Shrotriya, V.; Huang, J.; Yao, Y.; Moriarty, T.; Emery, K.; Yang, Y. High-Efficiency Solution Processable Polymer Photovoltaic Cells by Self-Organization of Polymer Blends. *Nat. Mater.* **2005**, *4*, 864–868.